Eur. Phys. J. D **16**, 87–90 (2001)

THE EUROPEAN
PHYSICAL JOURNAL D
EDP Sciences

Collision-induced fragmentation and neutralization of methanol cluster cations

W. Christen[1,a] and U. Even[2]

[1] Humboldt-Universität zu Berlin, Institut für Physikalische und Theoretische Chemie, Bunsenstr. 1, 10117 Berlin, Germany
[2] Tel Aviv University, Sackler Faculty of Exact Sciences, School of Chemistry, Ramat Aviv, Tel Aviv 69978, Israel

Received 30 November 2000

Abstract. This contribution addresses the inelastic interaction of positively charged molecular cluster ions with a solid surface at kinetic energies up to 30 eV/molecule. We report experimental results on the scattering of mass-selected, protonated methanol cluster cations $(CH_3OH)_nH^+$, $n = 4-32$, off a diamond-coated silicon surface. In particular we provide fragment size distributions of methanol cluster ions following their impact on the target, as well as surface-induced neutralization probabilities of methanol cluster ions as a function of the size and the kinetic energy of the parent clusters.

PACS. 34.30.+h Intramolecular energy transfer; intramolecular dynamics; dynamics of van der Waals molecules – 34.50.-s Scattering of atoms and molecules – 34.70.+e Charge transfer – 36.40.-c Atomic and molecular clusters – 61.46.+w Nanoscale materials: clusters, nanoparticles, nanotubes, and nanocrystals – 81.16.-c Methods of nanofabrication and processing – 82.30.-b Specific chemical reactions; reaction mechanisms – 82.40.-g Chemical kinetics and reactions: special regimes and techniques

1 Introduction

During the collision of a weakly-bound molecular cluster with a solid substrate, the initially directed kinetic energy of the cluster will be thermalized rapidly by collisions of the molecules of the cluster with each other and with the atoms of the solid surface. This sudden, impact-induced redistribution of the cluster translational energy may lead to a variety of processes, including the collision-induced dissociation of inter- and intramolecular bonds, charge exchange processes between the projectile and the target, and both homogeneous and heterogeneous chemical reactions.

Inelastic cluster-surface collisions have received considerable attention, because — *inter alia* — these experiments can provide large amounts of internal excitations to the impacting clusters, on a sub-picosecond time-scale. This way, for the first time it is possible to investigate the dynamics and the reactivity of physical and chemical processes under extreme temperatures and pressures [1–29] under controlled and clean, well-defined conditions. So far, however, due to the inherent experimental complexity, investigations of chemical processes taking place during cluster-surface collisions are rare [30–37]. Obviously, more detailed experimental results are necessary for a deeper understanding of the ultrafast chemical dynamics in cluster-surface collisions.

The main goal of this report is to examine the possibility of extracting energetic information concerning the stability of the clusters from the measurement of energy-resolved fragment ion distributions of size-selected cluster ions. We present a systematic, experimental study of the collision-induced fragmentation and neutralization of positively charged clusters of a simple organic molecule, colliding with a solid, nonreactive diamond surface at kinetic energies up to 30 eV/molecule. Energy-resolved time-of-flight mass spectrometry is used to obtain quantitative fragment ion abundances of mass-selected, protonated methanol cluster ions, as a function of the cluster size and the impact energy.

2 Experiment

An overview of the experimental set-up used for our investigations is shown in Fig. 1. It consists mainly of a pulsed cluster ion source, a primary time-of-flight mass spectrometer, two pulsed mass-gates and an ultrahigh vacuum target collision chamber containing a secondary time-of-flight mass spectrometer for fragment analysis.

Positively charged cluster ions are efficiently generated by pulsed electron ionization (70−120 eV, 4−10 μs voltage pulse) of the supersonically expanded gaseous methanol, diluted in a carrier gas, typically a mixture of 30% neon and 70% helium. The jet source consists of a newly designed, home-built pulsed valve [40]. Operation conditions are 10−15 μs pulse width, 10 Hz repetition rate, 1−5 MPa stagnation pressure and 330 K stagnation temperature. The resulting ions are collimated and passed to the

---

[a] e-mail: `christen@chemie.hu-berlin.de`

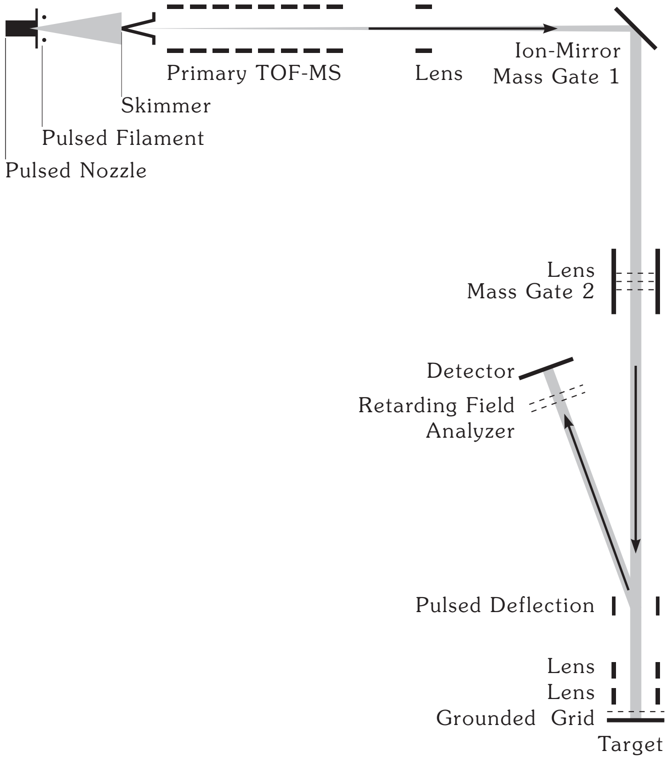

Fig. 1. Schematic view of the experimental setup. For more details see [38,39].

primary time-of-flight mass spectrometer, where they are accelerated to a translational energy of about 2 keV. A first mass selection of the beam is achieved by pulsing the high voltage applied at a planar ion mirror, at the correct timing, deflecting a single cluster size by 90° into the UHV scattering chamber. For improved mass resolution a second mass gate has been added, at a distance $\simeq 250$ mm from the ion mirror. The cluster ions are directed along the surface normal of a silicon target, which is coated with an electrically conductive ($\simeq 80\ \Omega\ \mathrm{cm}^{-1}$), $\simeq 10\ \mu$m thick p-type diamond film [41] and heated to about 400 K. Prior to surface-impact the cluster ions are decelerated to the desired collision energy using a strong retarding field between a grounded grid and the target surface, to which a high voltage is applied. The same high field ($\simeq 10^6\ \mathrm{V\,m}^{-1}$) that decelerates the incoming cluster ions is also used to efficiently collect and reaccelerate scattered ions. It allows a mass analysis of fragment ions through their time-of-flight from the target to the detector. The second time-of-flight mass spectrometer is equipped with a retarding field energy analyzer in front of the ion detector to determine the kinetic energy distribution of ions. This measurement is accomplished by a mass-specific integration of transmitted ions as a function of the retarding voltage of the analyzer. As has been shown previously [39], the measured data can be fitted accurately to an error function, which corresponds to a Gaussian energy distribution of the beam. The Gaussian maximum is taken as the mean kinetic energy of the ions. The relative translational energy spread of the primary cluster beam is less than 1%.

3 Data evaluation

Fragmentation and neutralization are common phenomena observed in experiments investigating the interaction of cluster ions with solid surfaces. Unfortunately it is quite difficult to separate both processes, because both of them strongly depend on the collision energy, and because both processes result in a very similar experimental outcome, *i.e.* the sudden drop of the parent cluster ion intensity with increasing collision energy. Moreover, the physical picture is convoluted by the finite width of the energy distribution of the impinging cluster ion beam. A correct interpretation of the measured data thus is a formidable task. This is especially true because most theoretical investigations tend to neglect the ionic nature of the charged particles used in the experiments.

The experimental difficulty to discriminate between fragmentation and neutralization arises because, due to the finite width of the initial energy distribution, the secondary time-of-flight mass spectrometer can not distinguish between cluster ions that have been *scattered intact* from the target surface, and cluster ions that have been *reflected* elastically. Employing the electrostatic, retarding field analyzer it is, however, possible to separate both processes because of the additional knowledge of the energy distribution of the primary cluster ion beam: Suppose that all primary cluster ions, with a nearly Gaussian kinetic energy distribution (see Ref. [38]), would hit the target and get neutralized on impact, the energy-dependent yield of parent cluster ions would be given by an integrated Gauss-distribution (error-function), as visualized by the dotted curve in Fig. 2. The difference of the mass spectrometric measurement (open circles) to the contribution of surface-induced neutralization of parent cluster ions (dotted curve) then yields the upper limit of intact scattered parent cluster ions, as shown by the thin continuous line in Fig. 2. It turns out that scattered ions are best represented by an asymmetrical distribution function, commonly known as Weibull-distribution.

4 Results

Fig. 3 shows the fragmentation pattern of protonated clusters of 4, 12, and 20 methanol molecules as a function of the collision energy per molecule. Two features are of special interest here: First, it is evident that the width of the disappearing parent cluster ion signal is significantly narrower for larger clusters. Second, while for small parent cluster ions the relative fragment ion abundances amount only to a few percent, the fragment ion yield increases remarkably with cluster size. This is shown in more detail in Fig. 4, where the relative fragment ion abundances of protonated methanol cluster ions $(\mathrm{CH_3OH})_n\mathrm{H}^+$, $n = 4$, $n = 12$, $n = 20$, and $n = 28$, have been summed to obtain the total fragment ion yield. Note that for larger clusters more fragment ions than parent cluster ions can be detected.

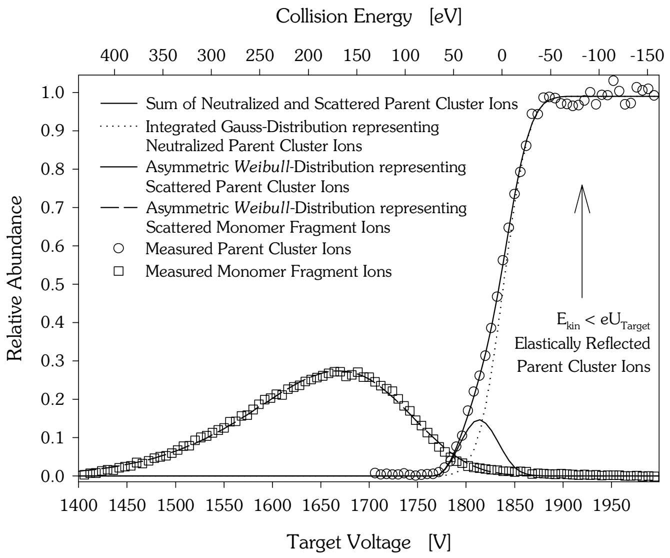

Fig. 2. Relative ion abundances for the surface collision of protonated methanol cluster ions $(CH_3OH)_{20}H^+$ with the diamond-coated silicon target. The measured ion signal is integrated for each mass and plotted as a function of the target voltage. For clarity only the parent cluster ion and the monomer fragment ion are shown in this figure. Target voltages higher than the kinetic energy of the incident cluster ions causes them to be reflected elastically, *i.e.* without impacting the target; this allows the detection of the primary cluster beam. The collision energy is given by the difference between the mean kinetic energy of the impinging ions and the target voltage. Ion intensities have been normalized to the intensity of incoming parent cluster ions and have been scaled to account for the velocity-dependent ion detection efficiency [42].

5 Summary

We have presented experimental results of the surface-induced fragmentation of positively charged, protonated methanol cluster ions, showing a pronounced transition from the intact parent cluster to complete fragmentation (*shattering* [43–45]) as a function of the collision energy. We emphasize the absence of any fragment ions with intermediate sizes or sizes close to the original parent cluster ion. A similar behavior has been observed for other hydrogen-bonded ion-clusters such as acetone, ammonia, and water.

The knowledge of the kinetic energy distribution of the impacting cluster ions allows us to distinguish between neutralized and back-scattered parent cluster ions and thus to give an upper limit for the survival probability of the impinging cluster ions. It turns out that a maximum of $\simeq 30\%$ of the parent cluster ions can survive the collision intact, and most parent cluster ions are neutralized on surface impact. Thus the sudden drop of the parent cluster ion intensity can be understood as originating mostly from an electron transfer from the target to the colliding cluster.

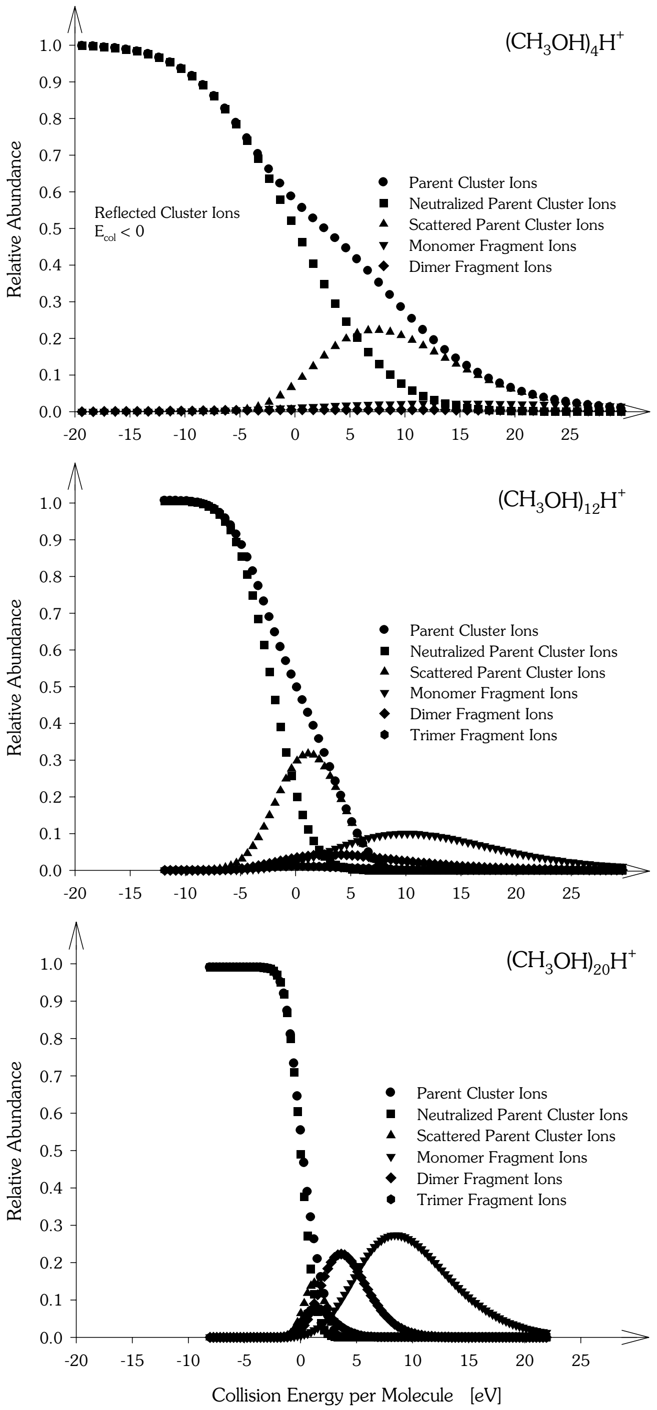

Fig. 3. Yield of charged cluster fragments due to the collision of protonated methanol cluster ions $(CH_3OH)_nH^+$ with the diamond target, for $n = 4$, $n = 12$, and $n = 20$.

The total fragment ion yield exhibits its maximum at intermediate collision energies of $\simeq 4.75$ eV/molecule and increases with cluster size. It leads us to conclude that, in analogy to Ref. [46], the proton is solvated in the cluster, and thus is better shielded from the conductive target surface.

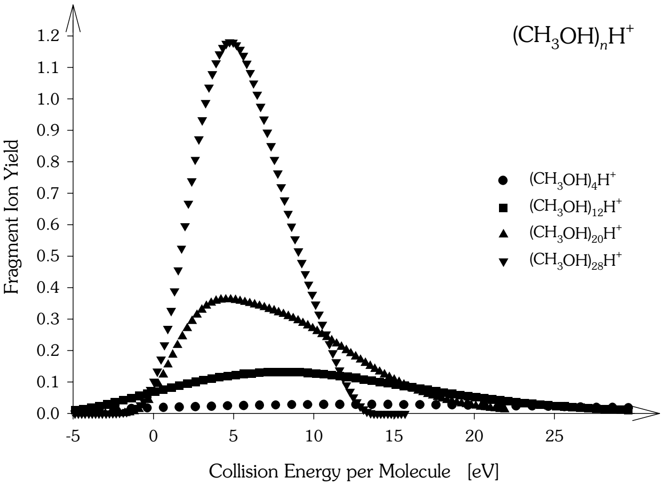

Fig. 4. Total fragment ion yield of protonated methanol cluster ions $(CH_3OH)_nH^+$, for $n = 4$, $n = 12$, $n = 20$, and $n = 28$, obtained by summation of the relative ion yields of the dominant fragment ions (monomer, dimer, trimer, tetramer).

We gratefully acknowledge financial support by a grant from GIF.

References

1. M.H. Shapiro, T.A. Tombrello, Phys. Rev. Lett. **65**, 92 (1990).
2. M.H. Shapiro, T.A. Tombrello, Nucl. Instrum. Meth. Phys. Res. B **58**, 161 (1991).
3. M.H. Shapiro, T.A. Tombrello, Mod. Phys. Lett. B **5**, 341 (1991).
4. M.H. Shapiro, T.A. Tombrello, Nucl. Instrum. Meth. Phys. Res. B **66**, 317 (1992).
5. C.L. Cleveland, U. Landman, Science **257**, 355 (1992).
6. M.H. Shapiro, T.A. Tombrello, Phys. Rev. Lett. **68**, 1613 (1992).
7. U. Even, I. Schek, J. Jortner, Chem. Phys. Lett. **202**, 303 (1993).
8. H.-P. Cheng, U. Landman, Science **260**, 1304 (1993).
9. H.-P. Cheng, U. Landman, J. Phys. Chem. **98**, 3527 (1994).
10. M.H. Shapiro, G.A. Tosheff, T.A. Tombrello, Nucl. Instrum. Meth. Phys. Res. B **88**, 81 (1994).
11. I. Schek, T. Raz, R.D. Levine, J. Jortner, J. Chem. Phys. **101**, 8596 (1994).
12. T. Raz, I. Schek, M. Ben-Nun, U. Even, J. Jortner, R.D. Levine, J. Chem. Phys. **101**, 8606 (1994).
13. T. Raz, R.D. Levine, Chem. Phys. Lett. **226**, 47 (1994).
14. T. Raz, R.D. Levine, J. Am. Chem. Soc. **116**, 11167 (1994).
15. T. Raz, R.D. Levine, J. Phys. Chem. **99**, 7495 (1995).
16. T. Raz, R.D. Levine, J. Phys. Chem. **99**, 13713 (1995).
17. T. Raz, R.D. Levine, Chem. Phys. Lett. **246**, 405 (1995).
18. Z.Y. Pan, M. Hou, Nucl. Instrum. Meth. Phys. Res. B **102**, 317 (1995).
19. Z. Insepov, I. Yamada, Nucl. Instrum. Meth. Phys. Res. B **112**, 16 (1996).
20. S.J. Timoner, M.H. Shapiro, T.A. Tombrello, Nucl. Instrum. Meth. Phys. Res. B **114**, 20 (1996).
21. M. Gupta, E.A. Walters, N.C. Blais, J. Chem. Phys. **104**, 100 (1996).
22. I. Schek, J. Jortner, J. Chem. Phys. **104**, 4337 (1996).
23. I. Schek, J. Jortner, T. Raz, R.D. Levine, Chem. Phys. Lett. **257**, 273 (1996).
24. T. Raz, R.D. Levine, Chem. Phys. **213**, 263 (1996).
25. M. Moseler, J. Nordiek, H. Haberland, Phys. Rev. B **56**, 15439 (1997).
26. G. Betz, W. Husinsky, Nucl. Instrum. Meth. Phys. Res. B **122**, 311 (1997).
27. L. Qi, S.B. Sinnott, J. Phys. Chem. B **101**, 6883 (1997).
28. L. Qi, S.B. Sinnott, J. Vac. Sci. Technol. A **16**, 1293 (1998).
29. L. Qi, S.B. Sinnott, Nucl. Instrum. Meth. Phys. Res. B **140**, 39 (1998).
30. R.L. Whetten, M.L. Homer, X. Li, F.E. Livingston, P.M. St. John, R.D. Beck, Ber. Bunsenges. Phys. Chem. **96**, 1120 (1992).
31. P.M. St. John, R.D. Beck, R.L. Whetten, Phys. Rev. Lett. **69**, 1467 (1992).
32. P.M. St. John, R.D. Beck, R.L. Whetten, Z. Phys. D **26**, 226 (1993).
33. S.A. Klopcic, M.F. Jarrold, J. Chem. Phys. **106**, 8855 (1997).
34. W. Christen, U. Even, J. Phys. Chem. A **102**, 9420 (1998).
35. W. Christen, U. Even, Eur. Phys. J. D **9**, 29 (1999).
36. C. Mair, T. Fiegele, F. Biasioli, Z. Herman, T.D. Märk, J. Chem. Phys. **111**, 2770 (1999).
37. C. Mair, T. Fiegele, F. Biasioli, J.H. Futrell, Z. Herman, T.D. Märk, Int. J. Mass Spectrom. **188**, L1 (1999).
38. W. Christen, U. Even, T. Raz, R.D. Levine, Int. J. Mass Spectrom. Ion Proc. **174**, 35 (1998).
39. W. Christen, U. Even, T. Raz, R.D. Levine, J. Chem. Phys. **108**, 10262 (1998).
40. U. Even, J. Jortner, D. Noy, N. Lavie, C. Cossart-Magos, J. Chem. Phys. **112**, 8068 (2000).
41. General Vacuum Inc., Cleveland, OH 44105, P.O. Box 605204.
42. H. Yasumatsu, S. Koizumi, A. Terasaki, T. Kondow, J. Chem. Phys. **105**, 9509 (1996).
43. T. Raz, U. Even, R.D. Levine, J. Chem. Phys. **103**, 5394 (1995).
44. E. Hendell, U. Even, T. Raz, R.D. Levine, Phys. Rev. Lett. **75**, 2670 (1995).
45. T. Raz, R.D. Levine, J. Chem. Phys. **105**, 8097 (1996).
46. H. Yasumatsu, A. Terasakia, T. Kondow, Int. J. Mass Spectrom. Ion Proc. **174**, 297 (1998).